

First experiences with RTTOV8 for assimilating AMSU-A data in the DMI 3D-Var data assimilation system

Bjarne Amstrup

E-mail: bja@dmi.dk

Danish Meteorological Institute

Lyngbyvej 100, DK-2100 Copenhagen Ø, Denmark

Abstract

(A)TOVS¹ data over open sea have been operationally assimilated into the DMI-HIRLAM² system since December 2002 after long tests in a pre-operational setup.

The forward model used operationally at DMI to calculate model derived brightness temperatures for ATOVS data is RTTOV7³ developed in the Numerical Weather Prediction SAF⁴ project setup by EUMETSAT⁵. November 2004, RTTOV8 was released and has subsequently been implemented in HIRVDA⁶ at DMI. Here we present comparisons between results from using RTTOV7 (with FASTEM⁷⁻²) and RTTOV8 (with FASTEM-3). The coefficient files presently available for RTTOV8 use RTTOV7 optical depth predictors so the main difference is the FASTEM version.

This study shows essentially neutral impact by changing from RTTOV7 to RTTOV8.

The statistics for brightness temperatures from channels 1-3 and to some extent from channel 4 (these channels are essentially not used in the analysis) when compared to model derived brightness temperatures are very different in the two set-ups and is the result of the change in surface emissivity calculations.

Introduction

(A)TOVS AMSU-A⁸ level 1c data (brightness temperatures) over open sea have been operationally assimilated into the DMI-HIRLAM system since December 2002 after long tests in a pre-operational setup. Impact studies (e.g., Amstrup, 2001; Schyberg et al., 2003; Amstrup, 2002; Amstrup, 2003; Amstrup, 2004; Amstrup and Mogensen, 2004) have demonstrated the

¹(Advanced) TIROS Operational Vertical Sounder

²Danish Meteorological Institute - High Resolution Limited Area Model

³Radiative Transfer model for TOVS, release 7

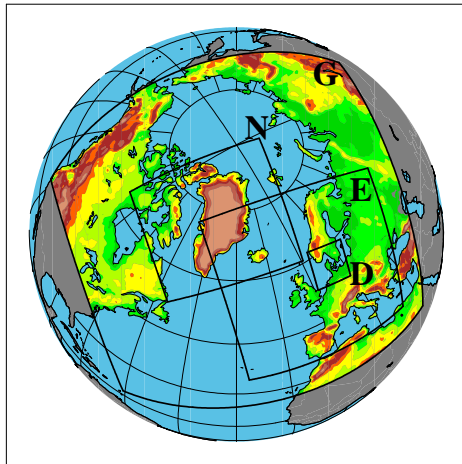
⁴Satellite Application Facility

⁵European organisation for the exploitation of METeorological SATellites

⁶HIRLAM Variational Data Assimilation

⁷FAST Emissivity Model

⁸Advanced Microwave Sounding Unit-A



Model Identification	G	N	E	D
grid points (mlon)	202	194	272	182
grid points (mlat)	190	210	282	170
No. of vertical levels	40	40	40	40
horizontal resolution	0.45°	0.15°	0.15°	0.05°
time step (dynamics)	120 s	50 s	50 s	18 s
time step (physics)	360 s	300 s	300 s	216 s

Figure 1: The DMI-HIRLAM regions, geographical coverage and resolution specifications.

positive impact of these data in the HIRLAM 3D-Var system, in particular in winter periods. Initially only locally received NOAA16 AMSU-A data were used operationally since we had problems processing the locally received NOAA15 AMSU-A data. Later NOAA17 were added after an impact study (Amstrup, 2003) and at the same time additional data from EARS⁹ were added. However, after the failure of NOAA17 we resolved the problem encountered previously with NOAA15 and after an OSE impact study (Amstrup, 2004) NOAA15 AMSU-A data also became part of the operational suite. See Schyberg et al. (2003) for further details concerning the use of ATOVS data in the HIRLAM 3D-Var system.

The operational system has always used RTTOV7 (Saunders et al., 1999; Matricardi et al., 2004) as the radiative transfer model to derive brightness temperatures from the forecast model parameters. November 2004 a new version of RTTOV, RTTOV8, became available. It includes, along many other changes, a new version of FASTEM which should improve the model derived brightness temperatures for the channels “seeing” the surface, i.e., in particular channels 1-4. These channels are presently not used in the DMI-HIRLAM 3D-Var since the observation errors assigned to these channels are very large. Here, we present some statistics and results from a parallel experiment from January 2005 using either RTTOV7 or RTTOV8 in the 3D-Var analyses.

Set-up of the experiments

In this study a local version of the HIRLAM (Sass et al., 2002; Amstrup et al., 2003) was used – it is the former operational model and is still run in parallel with the new operational setup. The model is regional and nested with four different regions (see figure 1 for an illustration and table of the position and resolution for the various models). The largest area model (DMI-HIRLAM-G) has lateral boundaries from ECMWF¹⁰, whereas the inner models have lateral boundaries from their surrounding HIRLAM model. The DMI-HIRLAM analysis and forecasting system consists of a 3 dimensional variational data analysis system (Gustafsson et al., 2001; Lindskog et al., 2001) with an assimilation window of 3 hours, and a forecast model with 40 vertical levels reaching the 10 hPa pressure level - above this a climatological model is applied for data needed in the radiative transfer model.

⁹EUMETSAT ATOVS Retransmission Service

¹⁰European Centre for Medium-Range Weather Forecasts

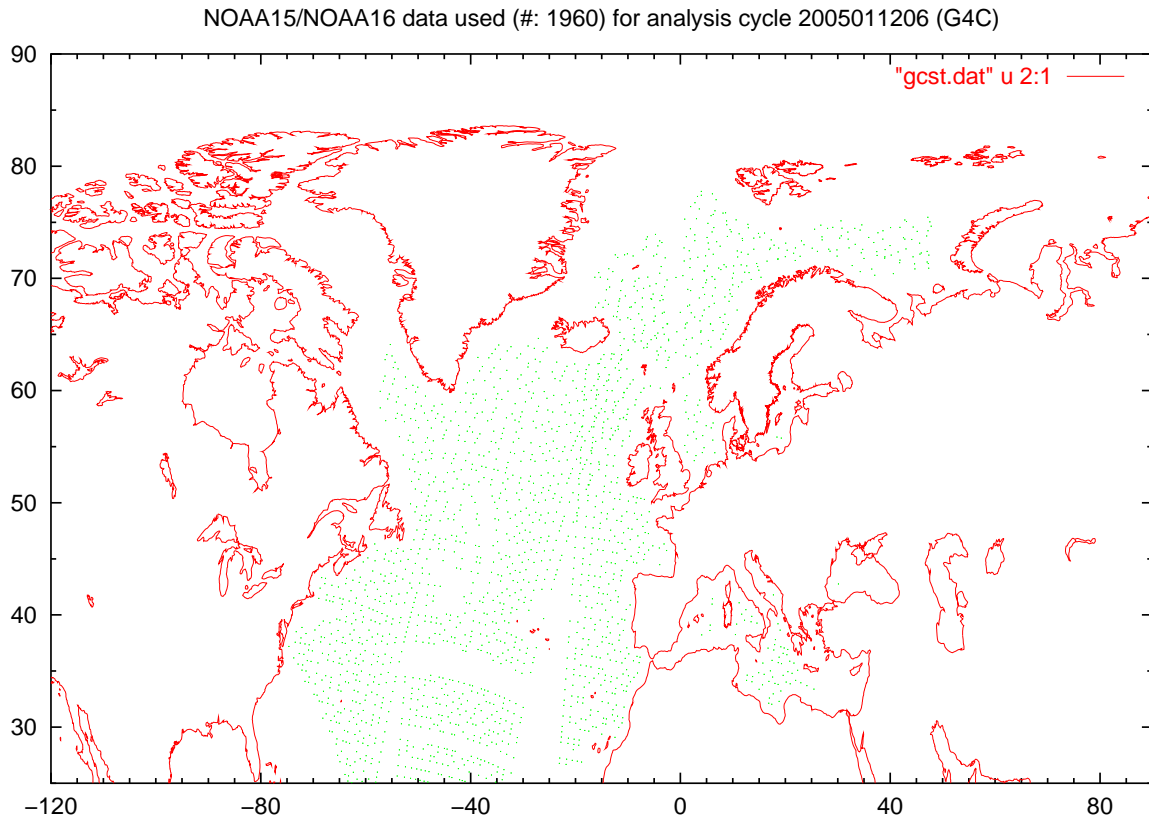


Figure 2: Positions (with green dots) of active (after data thinning) NOAA15/NOAA16 data used in the analysis valid on 06 UTC 20050112.

In the “Observing System Experiment” made here we used January 2005 with 3 hour data assimilation cycles (using the HIRLAM 3D-VAR system) and a 48 hour gridpoint forecast with the DMI-HIRLAM-G and DMI-HIRLAM-E models. In the HIRLAM 3D-VAR system the following observation types (and observation quantities) were used: SYNOP, DRIBU, SHIP (pressure), TEMP (temperature, wind and specific humidity), PILOT (wind), AIREP (temperature and wind), QuikScat (near surface wind), AMV¹¹ (wind) from Meteosat-8 and NOAA15/NOAA16 AMSU-A level 1c brightness temperatures over open sea. Figure 2 shows an example for the 06 UTC cycle on January 12th with very good coverage of AMSU-A data in the Atlantic. The data were screened using the following checks: 1) Bad reporting practices, 2) Black list check, 3) First guess check, 4) Multi-level check, 5) RDB check, and 6) Redundancy check. The final thinning for AMSU-A data in DMI-HIRLAM was 0.9°.

Bias correction and error statistics

An important issue in the use of satellite radiances is bias correction. The variational analysis system implicitly assumes that observations have Gaussian error distributions and are bias free. For satellite radiances the “errors” compared to model derived radiances come from the observations itself as well as from the forecast model via the radiative transfer model and from the radiative transfer model itself. For bias-correction a Harris-Kelly (Harris and Kelly, 2001)

¹¹Atmospheric Motion Vectors

scheme with 7 predictors from the background model (model first guess) is used: **1**) a constant displacement, **2**) thickness between 1000 hPa and 300 hPa, **3**) thickness between 200 hPa and 50 hPa, **4**) the surface temperature, **5**) the integrated water vapor content per area from the surface up to the top of the atmosphere, **6**) the square of the observation zenith angle and **7**) the observation zenith angle. For bias statistics locally available data from a 5.5 month period from June 1st to November 15th was used. This is the same period that was used to make the operationally bias correction coefficients (made after the interruption of NOAA17 AMSU-A data in late October 2003). In order to be sure that the same set of data is used as basis, the coefficients were recalculated using RTTOV7 as well. Figures 3 and 4 show the number of brightness temperature innovations (observed minus RTTOVx model derived from a 3 h forecast) in 0.1 K intervals for channels 4 through 10 for NOAA15 and NOAA16 using RTTOV7 or RTTOV8. Overlaid is the best fit (smallest root mean square (rms) value) Gaussian distribution. The left hand sides show the raw observational data and the right hand sides show the bias corrected observational data. The figures clearly show that the “shoulders” in the raw data essentially is removed in the bias corrected data and also that the width of the best fit Gaussian distributions are reduced for most of the channels in the latter. The biases has also changed to values very close to 0.

The initial studies that were done for NOAA16 (Schyberg et al., 2003) showed a considerable latitude dependency of the scatter of the observed versus model derived brightness temperatures. Accordingly, the bias corrections have been divided into three latitude bands in the operational implementations. For this study the limits are: south of 45°N; between 45°N and 65°N; and north of 65°N. Figure 5 shows the statistics for the difference between observed and first guess derived brightness temperatures for NOAA15 and NOAA16 AMSU-A data. In this figure the divisions in latitude bands are done so that approximately the same numbers are used in the statistics for each band. Note that the divisions are not the same for NOAA15 and NOAA16 data. This is due to the available data at DMI in the period for which the bias correction coefficients were made. Some latitude dependency can be seen in some of the channels. For the first 4 channels there is also a considerable difference in the bias statistics between RTTOV8 and RTTOV7 derived brightness temperatures. For RTTOV8 the statistics for channel 4 are as good as for the other channels effectively used in the analysis system.

The observation error covariance matrix has been chosen diagonal with the same values for NOAA15 and NOAA16. The values for channels 1-3 (“surface channels”) and for channel 4 are so large that effectively only channels 5-10 are used (see table 1). Examples of the effect of bias correction for NOAA15 in the operational DMI-HIRLAM-G model are found in figures 6 and 7. These figures also show the benefit of using FASTEM3 (Figure 6, RTTOV8) instead of FASTEM2 (Figure 7, RTTOV7) for channels 3 and 4 in the raw data statistics and to a lesser extend in the bias corrected data.

Table 1: The values in the diagonal of the observation error covariance matrix.
All off-diagonal elements are 0.

channel	1	2	3	4	5	6	7	8	9	10
error (K ²)	900	900	900	90	0.35	0.35	0.35	0.35	0.70	1.40

Results from “impact” study

The results from the “impact” study using either RTTOV7 or RTTOV8 in the 3D-Var data assimilation are given in terms of standard observation verification where forecast results are compared to standard SYNOP and radiosonde observations using an EWGLAM¹² station list. Results of forecasted 12h precipitation against observations from SYNOP stations at 06 UTC and 18 UTC are given in terms of standard contingency tables.

Figure 8 shows bias and root mean square (rms) errors for the surface variables 10 m wind, mslp (mean sea level pressure) and 2 m temperature; for the upper level variables temperature, wind speed and geopotential height at 850 hPa, 500 hPa and 250 hPa; and for relative humidity at 850 hPa and 500 hPa as function of forecast length. In this plot the G4C results should be compared to the G4E results and the D1C results should be compared to the D1E results. Basically the scores are very similar with some scores marginally better in one set of the runs and some scores marginally better in the other set of the runs. The most noticeable difference is the consistently better 10 m wind bias scores in the model runs using RTTOV8 than in the comparable model runs using RTTOV7.

Figure 9 shows the bias and rms of 10 m wind speed and 2 m temperature on an hourly basis for the DMI-HIRLAM-E runs for Danish stations that all provide observations every 10 min. January was very warm in Denmark with an average temperature 3.6°C above normal. This is probably part of the reason for the negative bias in temperature. For 2 m temperature the run (D1E) using RTTOV7 has slightly better scores than the run (D1C) using RTTOV8. For 10 m wind speed, the run using RTTOV8 has somewhat better bias scores.

Tables 2 and 3 show contingency tables of precipitation accumulated over 12 hours (from 6 to 18 hour or from 30 to 42 hour forecasts) using EWGLAM stations that do report 12 hours accumulated precipitation. The numbers in these tables are obtained by counting the number of observed and predicted precipitation amounts in each of five classes. The five precipitation classes are (precipitation amounts in mm): $P_1 < 0.2$, $0.2 \leq P_2 < 1.0$, $1.0 \leq P_3 < 5$, $5 \leq P_4 < 10$ and $P_5 \geq 10$. P is either F (forecast) or O (observation) in the tables. The “sum” rows and columns are the sums of the numbers in the given observation classes or forecast classes, respectively. Note that the observed values are uncorrected values. Thus, small observed precipitation values are most likely underestimated, and some “observed” 0 mm/12 h values may not be a real measurement at all, but merely a standard number used (this occasionally do happen for some Danish stations). The numbers in the tables are quite similar for the two set of runs, except for the O1/F1 class being better in 30 to 42 hour forecasts for the runs using RTTOV8.

Overall, the verification scores are neutral with respect to using RTTOV7 or RTTOV8 in the 3D-Var analysis system. However, the statistics show a possible benefit of using channel 4 in the analysis system when using RTTOV8.

Conclusions and future prospects

As expected the impact on the DMI-HIRLAM 3D-Var data assimilation system of changing the radiative transfer model from RTTOV7 to RTTOV8 is fairly small since the 3 “surface channels” 1-3 and also channel 4 essentially are not used and the main difference between the setups is the FASTEM version. However, more data is rejected in the run using RTTOV8. This is due to the different characteristics of channels 1 and 2 that are used for cloud cover rejection.

¹²European Working Group on Limited Area Model

Furthermore, the initial statistics for channel 4 is better when using RTTOV8 than when using RTTOV7 and the observation error should be reduced for this channel in order to benefit from the data.

The use of channels 6-10 over land and over sea-ice is presently under investigations using RTTOV8. For this, surface temperature and integrated water vapor content are not used as bias predictors. The 5 predictors used are the same as over open sea.

RTTOV8 is computationally more expensive than RTTOV7 on the DMI NEC SX-6 vector computer. The implementation of RTTOV8 was also more complicated and took much longer time than the implementation of RTTOV7. Nevertheless, RTTOV8 should also be part of the operational system in the near future.

References

- Amstrup, B. (2001). Impact of ATOVS AMSU-A radiance data in the DMI-HIRLAM 3D-Var analysis and forecasting system. DMI scientific report 01-06, Danish Meteorological Institute.
- Amstrup, B. (2002). Impact of ATOVS AMSU-A radiance data in the DMI-HIRLAM 3D-Var analysis and forecasting system - February 2002. In *HIRLAM Workshop Report of HIRLAM Workshop on Variational Data Assimilation and Remote Sensing*, pages 68–76.
- Amstrup, B. (2003). Impact of NOAA16 and NOAA17 ATOVS AMSU-A radiance data in the DMI-HIRLAM 3D-VAR analysis and forecasting system — January and February 2003. DMI scientific report 03-06, Danish Meteorological Institute.
- Amstrup, B. (2004). Impact of NOAA15 and NOAA16 ATOVS AMSU-A radiance data in the DMI-HIRLAM 3D-VAR data assimilation system – november and december 2003. *Hirlam Newsletter*, 45:235–247.
- Amstrup, B. and Mogensen, K. S. (2004). Observing system experiments with the DMI HIRLAM 3D-VAR data assimilation system in a winter and summer period in 2002. *unpublished results*.
- Amstrup, B., Mogensen, K. S., Nielsen, N. W., Huess, V., and Nielsen, J. W. (2003). Results from DMI-HIRLAM pre-operational tests prior to the upgrade in December 2002. DMI technical report 03-20, Danish Meteorological Institute.
- Gustafsson, N., Berre, L., Hörnquist, S., Huang, X.-Y., Lindskog, M., Navascués, B., Mogensen, K. S., and Thorsteinsson, S. (2001). Three-dimensional variational data assimilation for a limited area model. Part I: General formulation and the background error constraint. *Tellus*, 53A:425–446.
- Harris, B. A. and Kelly, G. (2001). A satellite radiance-bias correction scheme for data assimilation. *Quart. J. Roy. Meteorol. Soc.*, 127:1453–1468.
- Lindskog, M., Gustafsson, N., Navascués, B., Mogensen, K. S., Huang, X.-Y., Yang, X., Andræ, U., Berre, L., Thorsteinsson, S., and Rantakokko, J. (2001). Three-dimensional variational data assimilation for a limited area model. Part II: Observation handling and assimilation experiments. *Tellus*, 53A:447–468.
- Matricardi, M., Chevallier, F., Kelly, G., and Thépaut, J.-N. (2004). An improved general fast radiative transfer model for the assimilation of radiance observations. *Quart. J. Roy. Meteorol. Soc.*, 130:153–173.

- Sass, B. H., Nielsen, N. W., Jørgensen, J. U., Amstrup, B., Kmit, M., and Mogensen, K. S. (2002). The operational DMI-HIRLAM system - 2002 version. DMI technical report 02-05, Danish Meteorological Institute.
- Saunders, R., Matricardi, M., and Brunel, P. (1999). An improved fast radiative transfer model for assimilation of satellite radiance observations. *Quart. J. Roy. Meteorol. Soc.*, 125:1407–1425.
- Schyberg, H., Landelius, T., Thorsteinsson, S., Tvetter, F. T., Vignes, O., Amstrup, B., Gustafsson, N., Järvinen, H., and Lindskog, M. (2003). Assimilation of ATOVS data in the HIRLAM 3D-VAR system. *HIRLAM Technical Report*, 60.

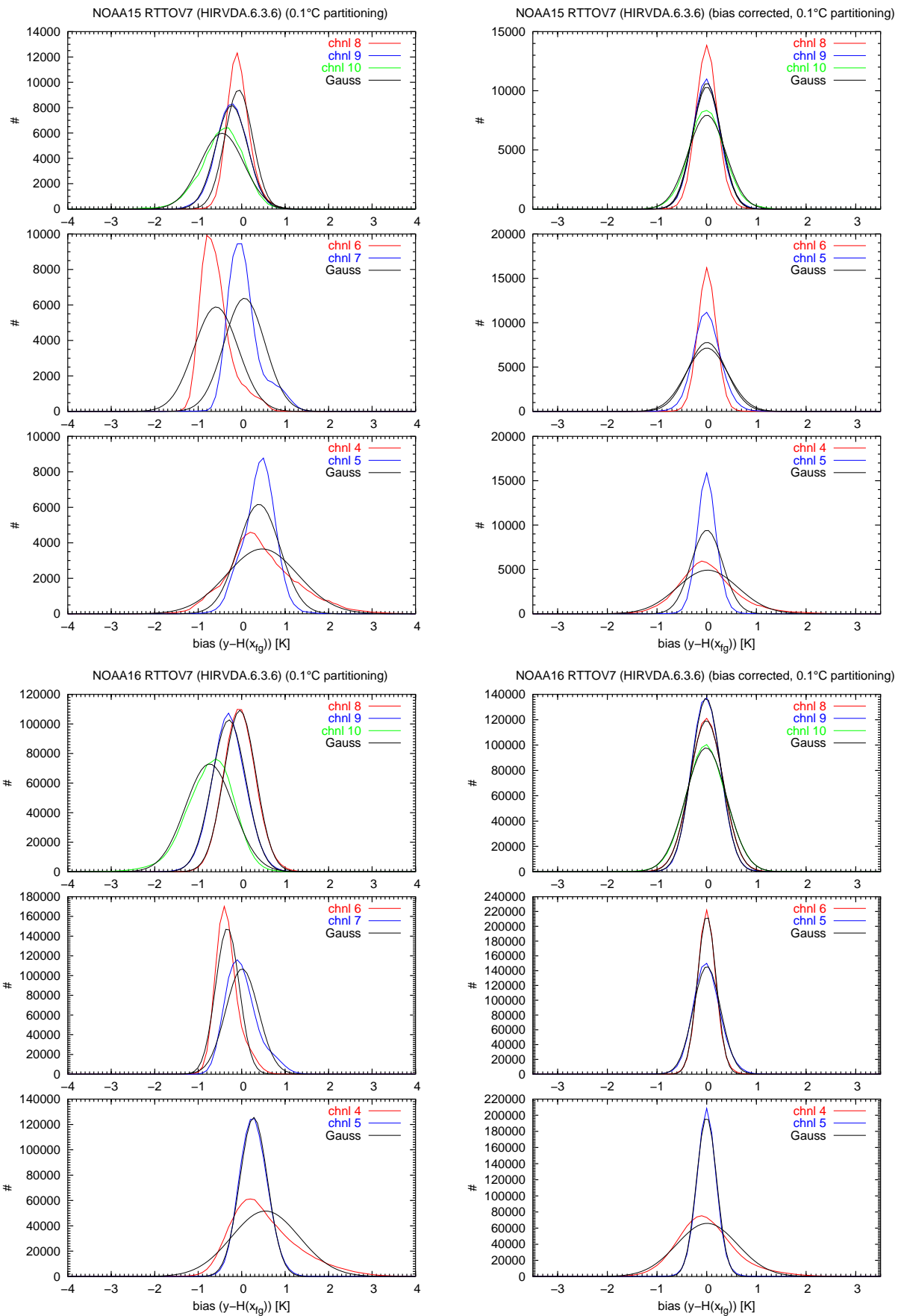


Figure 3: Statistics (observed minus first guess derived brightness temperatures) of NOAA15 AMSU-A (upper) and NOAA16 AMSU-A (lower) data for channels specified in the figures. Left is for raw data and right is for bias corrected data. RTTOV7 has been used for model derived brightness temperatures.

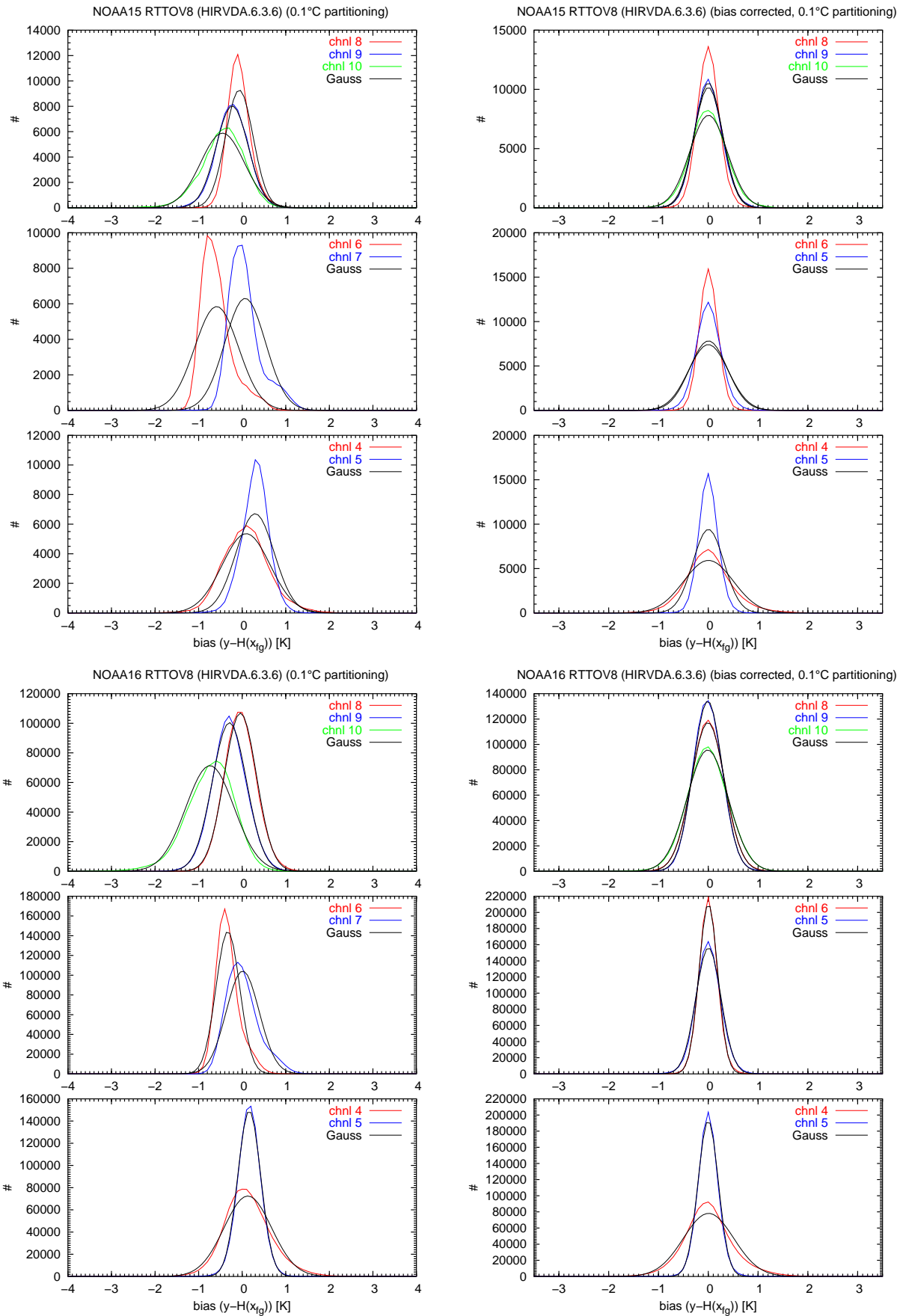


Figure 4: Statistics (observed minus first guess derived brightness temperatures) of NOAA15 AMSU-A (upper) and NOAA16 AMSU-A (lower) data for channels specified in the figures. Left is for raw data and right is for bias corrected data. RTTOV8 has been used for model derived brightness temperatures.

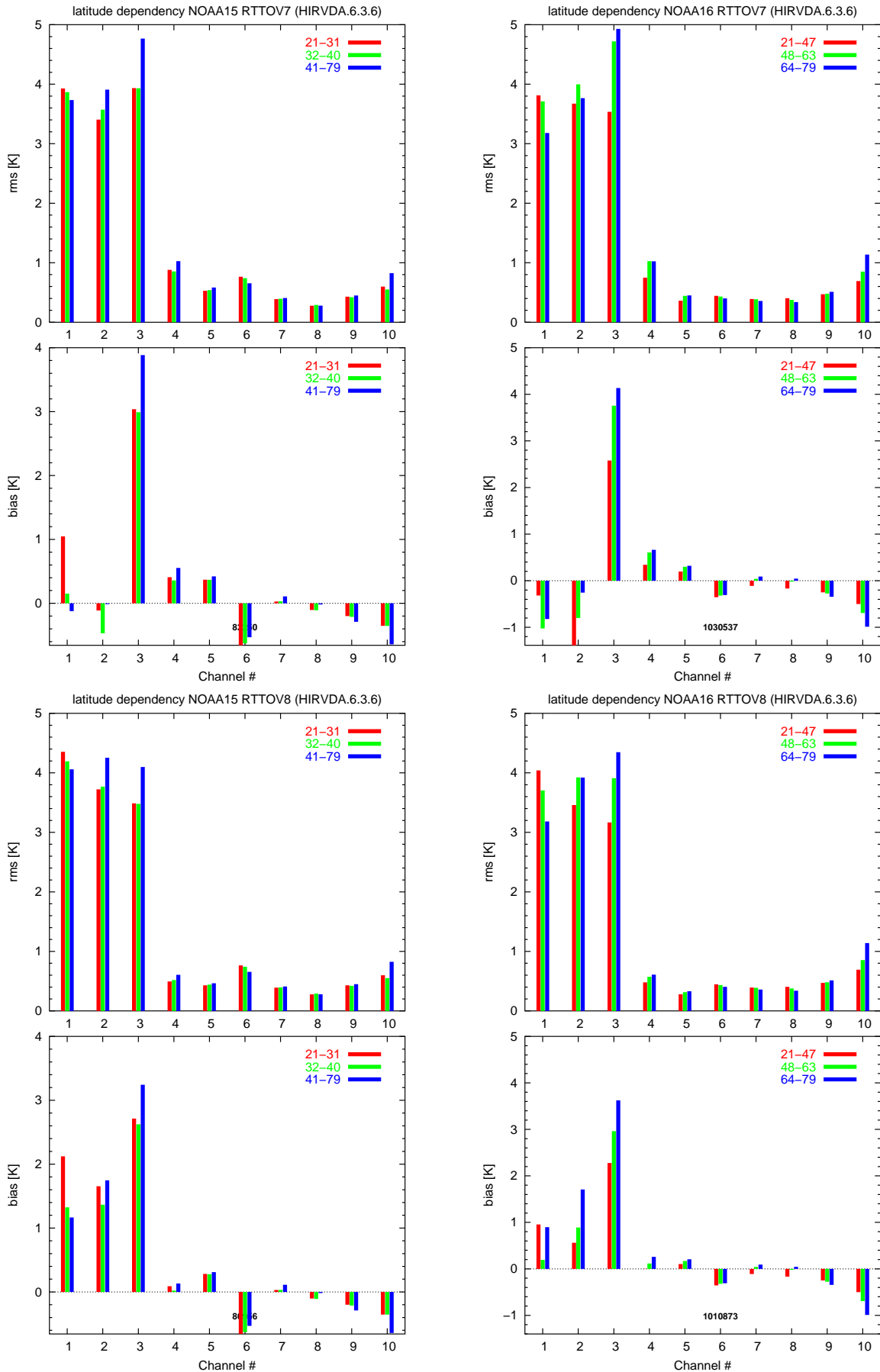


Figure 5: Statistics (observed minus first guess derived brightness temperatures) of NOAA15 AMSU-A (left) and NOAA16 AMSU-A (right) data for channels specified in the figures. RTTOV7 (upper) and RTTOV8 (lower) has been used for model derived brightness temperatures. Latitude dependency.

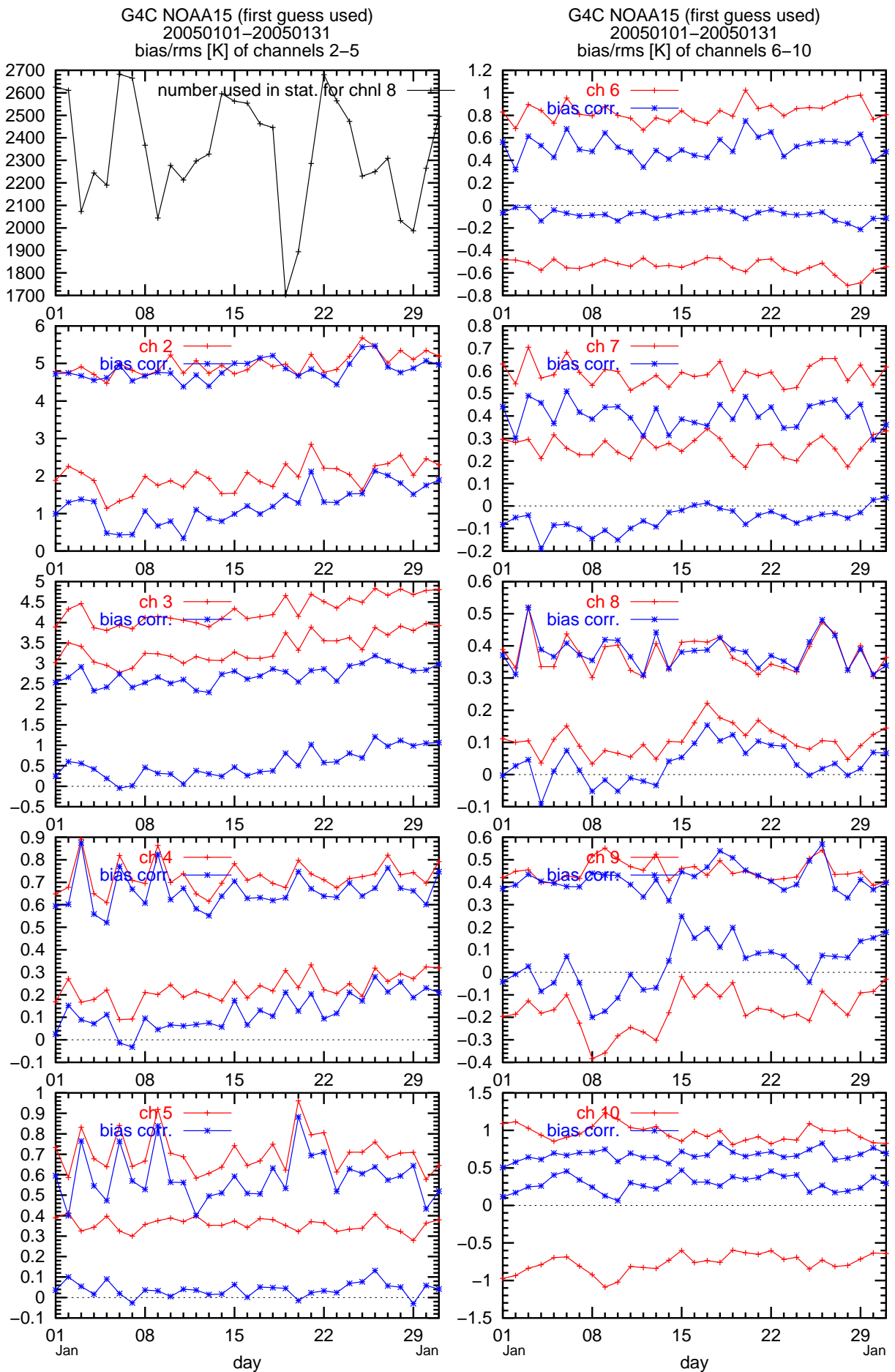


Figure 6: Daily bias- and rms-values (level 1c (OBS – FG) brightness temperature departure (in K) for NOAA15 AMSU-A channels 2-10 in January 2005. Red values for uncorrected and blue for bias corrected values. RTTOV-8 used and for DMI-HIRLAM-G area.

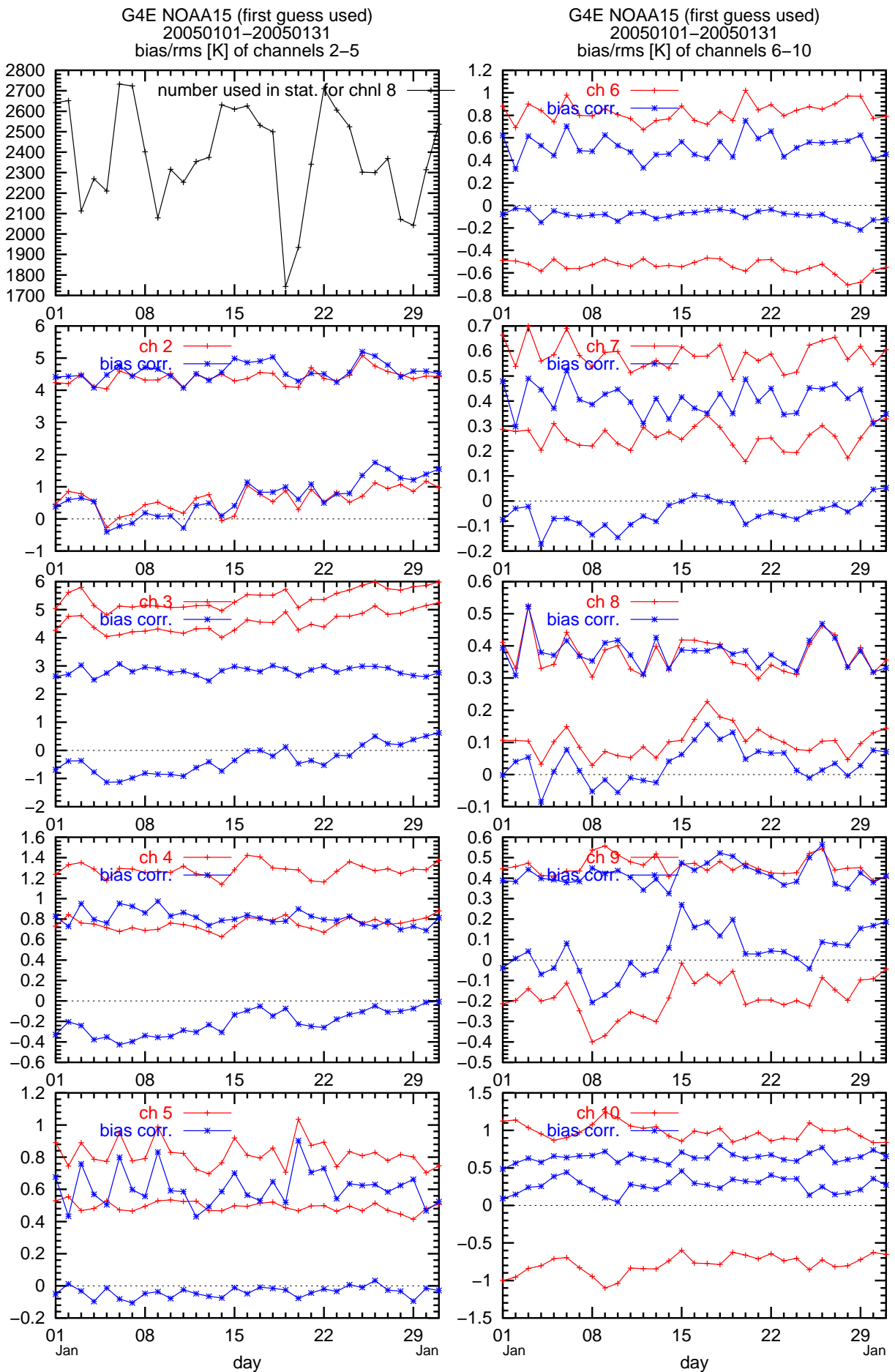


Figure 7: Daily bias- and rms-values (level 1c (OBS – FG) brightness temperature departure (in K) for NOAA15 AMSU-A channels 2-10 in January 2005. Red values for uncorrected and blue for bias corrected values. RTTOV-7 used and for DMI-HIRLAM-G area.

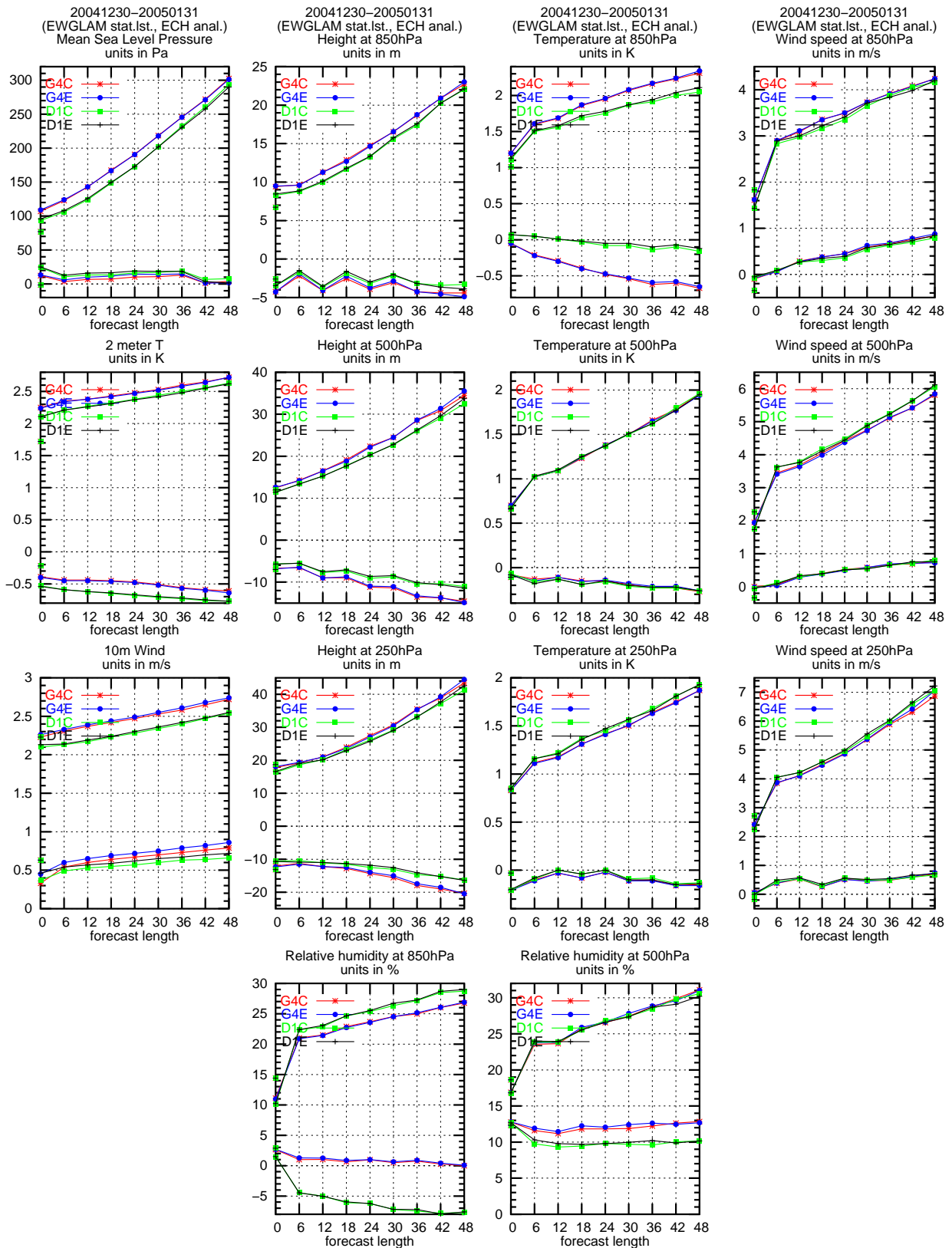


Figure 8: Observation verification against EWGLAM stations for parameters specified in the plot. G4E/G4C is DMI-HIRLAM-G area models and D1E/D1C is DMI-HIRLAM-E area models. The G4E/D1E run has used RTTOV7 and the G4C/D1C run has used RTTOV8.

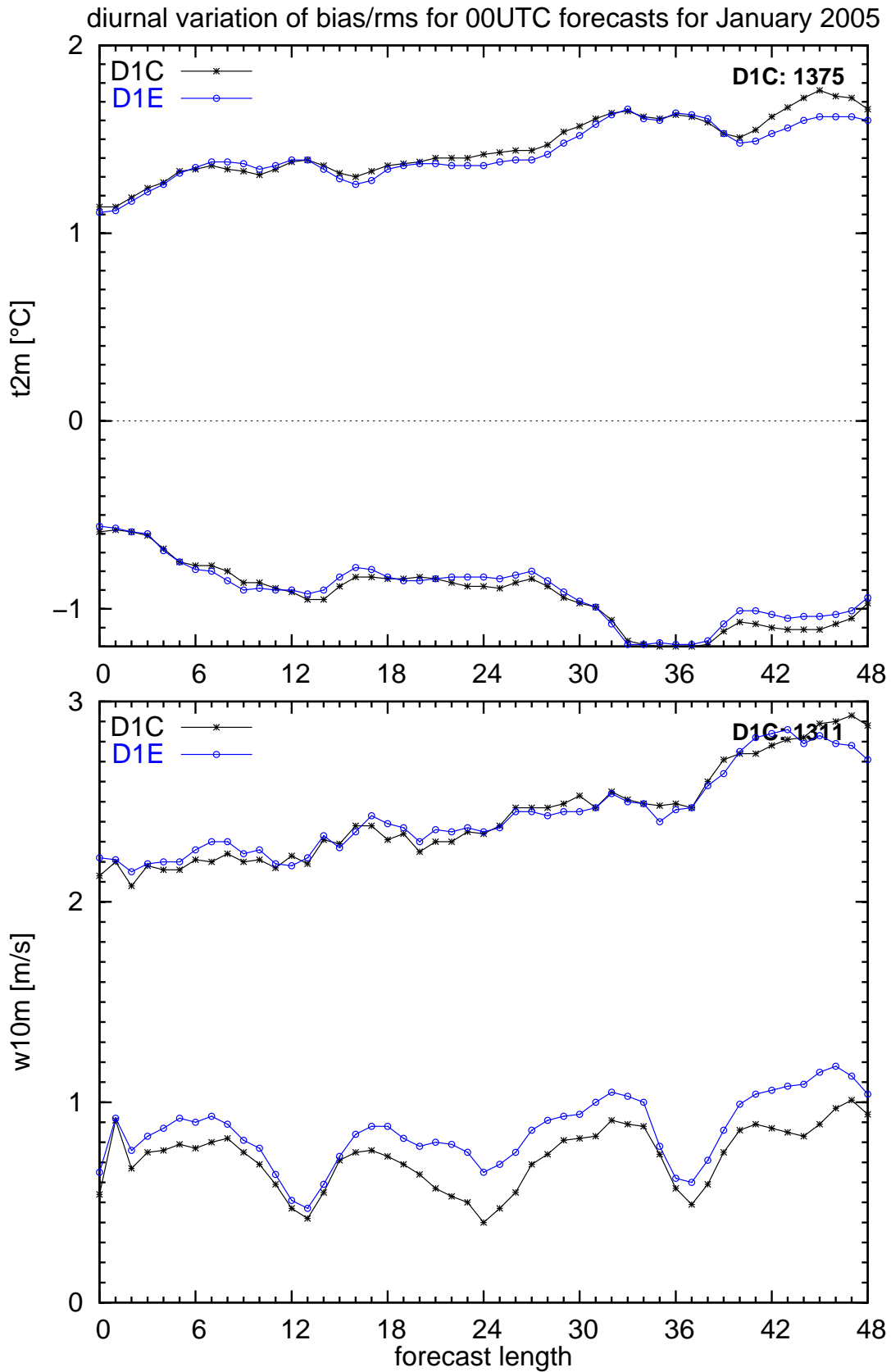


Figure 9: Average bias and rms values in January 2005 of 2m temperature (upper) and 10m wind speed (lower) as function of forecast length and the corresponding observations valid at the same time for a number of Danish stations for which observations are given (at least) once per hour. Only forecasts starting from 00UTC are included. The number in the upper right corner of each sub-figure indicates the average numbers of observations used in the calculations for each forecast length for D1C. D1C is the DMI-HIRLAM-E run with RTTOV8 and D1E is the DMI-HIRLAM-E run with RTTOV7.

Table 2: Contingency table(s) for 0501 (6–18 h forecasts). EWGLAM station list.

D1E (RTTOV7) 200501							D1C (RTTOV8) 200501						
$\frac{\text{obs} \rightarrow}{\downarrow \text{for}}$	O1	O2	O3	O4	O5	sum	$\frac{\text{obs} \rightarrow}{\downarrow \text{for}}$	O1	O2	O3	O4	O5	sum
F1	6867	336	83	23	26	7335	F1	6837	291	70	28	26	7252
F2	3501	1100	438	33	11	5083	F2	3532	1135	476	32	10	5185
F3	1244	1182	1720	322	67	4535	F3	1238	1194	1710	326	65	4533
F4	71	80	318	258	108	835	F4	75	78	295	247	113	808
F5	10	17	65	75	115	282	F5	11	17	73	78	113	292
sum	11693	2715	2624	711	327	18070	sum	11693	2715	2624	711	327	18070
%FO	59	41	66	36	35	56	%FO	58	42	65	35	35	56
G4E (RTTOV7) 200501							G4C (RTTOV8) 200501						
$\frac{\text{obs} \rightarrow}{\downarrow \text{for}}$	O1	O2	O3	O4	O5	sum	$\frac{\text{obs} \rightarrow}{\downarrow \text{for}}$	O1	O2	O3	O4	O5	sum
F1	6603	298	59	5	3	6968	F1	6683	305	67	5	3	7063
F2	3796	1190	513	49	11	5559	F2	3739	1196	542	48	16	5541
F3	1231	1140	1702	326	81	4480	F3	1197	1133	1671	356	82	4439
F4	57	76	301	254	125	813	F4	68	69	292	228	116	773
F5	6	11	49	77	107	250	F5	6	12	52	74	110	254
sum	11693	2715	2624	711	327	18070	sum	11693	2715	2624	711	327	18070
%FO	56	44	65	36	33	55	%FO	57	44	64	32	34	55

Table 3: Contingency table(s) for 0501 (30–42 h forecasts). EWGLAM station list.

D1E (RTTOV7) 200501							D1C (RTTOV8) 200501						
$\frac{\text{obs} \rightarrow}{\downarrow \text{for}}$	O1	O2	O3	O4	O5	sum	$\frac{\text{obs} \rightarrow}{\downarrow \text{for}}$	O1	O2	O3	O4	O5	sum
F1	6688	445	162	42	30	7367	F1	6805	434	165	49	32	7485
F2	3620	1028	537	57	18	5260	F2	3528	1030	521	44	20	5143
F3	1460	1189	1542	338	72	4601	F3	1435	1197	1572	344	82	4630
F4	117	97	334	211	103	862	F4	116	91	329	209	99	844
F5	24	25	59	73	103	284	F5	25	32	47	75	93	272
sum	11909	2784	2634	721	326	18374	sum	11909	2784	2634	721	326	18374
%FO	56	37	59	29	32	52	%FO	57	37	60	29	29	53
G4E (RTTOV7) 200501							G4C (RTTOV8) 200501						
$\frac{\text{obs} \rightarrow}{\downarrow \text{for}}$	O1	O2	O3	O4	O5	sum	$\frac{\text{obs} \rightarrow}{\downarrow \text{for}}$	O1	O2	O3	O4	O5	sum
F1	6166	324	101	21	7	6619	F1	6245	336	125	23	11	6740
F2	3930	1120	532	48	21	5651	F2	3872	1092	519	52	19	5554
F3	1691	1219	1640	361	111	5022	F3	1664	1233	1643	372	103	5015
F4	103	97	305	228	102	835	F4	105	99	287	214	113	818
F5	19	24	56	63	85	247	F5	23	24	60	60	80	247
sum	11909	2784	2634	721	326	18374	sum	11909	2784	2634	721	326	18374
%FO	52	40	62	32	26	50	%FO	52	39	62	30	25	50